Thermochimica Acta, 176 (1991) 89–98
Elsevier Science Publishers B.V., Amsterdam

THERMAL, STRUCTURAL AND ELECTRICAL STUDIES OF THE CHLORO AND BROMO COMPLEXES OF COBALT, COPPER AND ZINC WITH 3-METHYL-2-PHENYLPYRIDINE

J.R. ALLAN and K. TURVEY

Department of Applied Chemical and Physical Sciences, Napier Polytechnic, Edinburgh (Gt. Britain)

(Received 9 May 1990)

ABSTRACT

The chloro and bromo compounds of cobalt, copper and zinc with 3-methyl-3-phenylpyridine were prepared in ethanolic solution from which solid compounds were isolated. The suggested structure for the cobalt and zinc compounds is tetrahedral, while for the copper compounds it is tetragonal. The techniques of thermogravimetry and differential thermal analysis show that the compounds bis(3-methyl-2-phenylpyridine)cobalt(II) chloride and bis(3-methyl-2-phenylpyridine)zinc(II) chloride form intermediate compounds before their metal oxides are produced. The other compounds lose organic ligand followed by halogen to give the metal oxide. Electrical conductivities at room temperature and for heating to 70 °C were measured. The room temperature conductivity of the zinc complexes greatly exceeds (by a factor of about 10^4) that of the copper and cobalt complexes.

INTRODUCTION

The compound 3-methyl-2-phenylpyridine has one donor site for forming bonds with metal ions: the nitrogen atom of the aromatic ring.

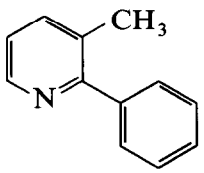

3-methyl-2-phenylpyridine ($C_{12}H_{10}N$).

In this paper we report studies of the chloro and bromo complexes of cobalt, copper and zinc with 3-methyl-2-phenylpyridine. Spectral and magnetic measurements have been used to characterise each metal complex and to interpret the type of coordination which takes place with the metal ion. The thermal decomposition of the complexes along with their electrical conductivity have been studied.

0040-6031/91/$03.50

EXPERIMENTAL

Preparation of complexes

The metal(II) halide (0.05 mol) was dissolved in a minimum of boiling ethanol. To the boiling ethanol solution was added 0.1 mol of 3-methyl-2-phenylpyridine with stirring. The resulting solution was heated for 5 min and then concentrated on a steam bath. The precipitated product was then isolated by filtration, washed with a minimum of ethanol and air dried.

Apparatus and measurements

The concentration of the metal ion was determined using a Perkin–Elmer 373 atomic absorption spectrophotometer. The carbon, hydrogen and nitrogen analyses were made using a Carlo Erba elemental analyser. The IR spectra were recorded using KBr discs over the wavenumber range 4000–600 cm^{-1} and polyethylene discs over the range 600–200 cm^{-1} on a Perkin–Elmer IR spectrophotometer model 598. The electronic spectra were recorded as solid diffuse reflectance spectra using a Beckmann Acta MIV spectrophotometer. Measurements of magnetic moments were made using the Gouy method with $Hg[Co(SCN)_4]$ as calibrant. The thermal analysis measurements were made on a Stanton Redcroft model STA 781 thermobalance. Thermogravimetry (TG) and differential thermal analysis (DTA) curves were obtained at a heating rate of 6 °C min^{-1} in static air. The 20–800 °C temperature range was studied in all cases.

The electrical conductivity (σ) was measured at room temperature for all of the complexes and, additionally, the temperature dependence of σ was measured for the three most conductive complexes.

A disc of diameter 13 mm and thickness in the range 0.66–1.22 mm was prepared for each complex by compressing powder under a force of 100 kN in a hydraulic press. Concentrically on the flat faces of the disc, a metal electrode of diameter 6.3 mm was provided by applying conductive silver paint through a mask. After the paint had dried and the disc had been kept for several days in a desiccator, it was placed in a holder in which the lower electrode made contact with a brass strip and contact to the upper electrode was through an aluminium pad held in place by a wire spring. Current (I) versus voltage (V) characteristics of the disc were obtained under direct current conditions using a Philip Harris pico/nano/micro ammeter and a digital voltmeter. The latter instrument was placed directly across the terminals of the variable voltage power supply so that the current registered by the ammeter was only that through the disc. Readings were obtained for increasing and then decreasing voltages in the same polarity, followed by similar readings under reversed polarity. The disc thickness, which is needed for determining the conductivity from the I versus V data, was obtained

using a micrometer. The temperature dependence of σ was obtained by recording the current through the disc as its temperature was raised from room temperature to approximately 70 °C under a constant applied voltage. For these measurements the disc, which was still in the holder, was placed in an electrically heated oven and temperature measurements were made with a calibrated copper–constantan thermocouple with its hot junction near the disc.

RESULTS AND DISCUSSION

The analytical results for the complexes are given in Table 1. These analyses agree with the formulae proposed for the compounds which are also given in Table 1.

TABLE 1

Analyses of compounds

Compound	Theory (%)				Found (%)			
	M	C	N	H	M	C	N	H
$Co(C_{12}H_{10}N)_2Cl_2$ [a]	12.63	61.82	6.00	4.32	12.41	61.42	5.54	4.07
$Co_3(C_{12}H_{10}N)_4Cl_6$ [b]	16.57	53.99	5.24	3.74	16.19	53.66	4.93	3.48
$Co(C_{12}H_{10}N)_2Br_2$ [a]	10.64	52.07	5.06	3.64	10.52	51.69	4.85	3.34
$Cu(C_{12}H_{10}N)_2Cl_2$ [a]	13.49	61.21	5.94	4.28	13.22	61.10	5.68	4.49
$Cu(C_{12}H_{10}N)_2Br_2$ [a]	11.38	51.64	5.01	3.61	11.12	51.44	4.66	3.42
$Zn(C_{12}H_{10}N)_2Cl_2$ [a]	13.82	60.98	5.92	4.26	13.39	60.48	5.56	4.14
$Zn(C_{12}H_{10}N)Cl_2$ [b]	21.39	47.12	4.58	3.27	21.22	47.34	4.66	3.39
$Zn(C_{12}H_{10}N)_2Br_2$ [a]	11.71	51.64	5.01	3.61	11.49	51.06	4.92	3.55

[a] Initial compound isolated from ethanolic solution.

[b] Intermediate compound produced by heating the corresponding initial compound.

TABLE 2

Electronic spectra and magnetic moments

Compound	Colour	Band position (cm^{-1})	d–d transition	μ (B.M.)
$Co(C_{12}H_{10}N)_2Cl_2$	Blue	7353	$^4A_2(F) \rightarrow {}^4T_1(F)$	4.78
		15823, 17241	$^4A_2(F) \rightarrow {}^4T_1(P)$	
$Co(C_{12}H_{10}N)_2Br_2$	Blue	6803	$^4A_2(F) \rightarrow {}^4T_1(F)$	4.56
		15290, 15873, 16667	$^4A_2(F) \rightarrow {}^4T_1(P)$	
$Cu(C_{12}H_{10}N)_2Cl_2$	Purple	18867	$^2B_1 \rightarrow {}^2A_1$	1.78
$Cu(C_{12}H_{10}N)_2Cl_2$	Green	16393	$^2B_1 \rightarrow {}^2A_1$	1.86

TABLE 3

Infrared spectroscopy (4000–200 cm^{-1})

Compound	Ring vibrations	ν(M–X)	ν(M–N) [a]
$C_{12}H_{10}N$	1577(s), 1420(s)		
$Co(C_{12}H_{10}N)_2Cl_2$	1585(s), 1433(s)	310(s), 330(s)	409(s)
$Co(C_{12}H_{10}N)_2Br_2$	1580(s), 1432(s)	240(m)	404(s)
$Cu(C_{12}H_{10}N)_2Cl_2$	1586(s), 1434(s)	279(m)	410(s)
$Cu(C_{12}H_{10}N)_2Br_2$	1582(s), 1430(s)	242(m)	412(s)
$Zn(C_{12}H_{10}N)_2Cl_2$	1588(s), 1435(s)	300(s)	406(s)
$Zn(C_{12}H_{10}N)_2Br_2$	1574(s), 1426(s)	260(m)	409(s)

[a] Ref. 3.

The electronic spectra and magnetic moments, both given in Table 2, would suggest that the cobalt ions in the chloro and bromo complexes are in a tetrahedral environment [1]. The broad absorption band between 16000 and 19000 cm^{-1} in the copper compounds is characteristic of a tetragonal structure [2]. The magnetic moment for each of the copper compounds is slightly higher than the spin only value of 1.73 B.M., suggesting the presence of some orbital contribution.

In Table 3 the main bands in the IR spectra are listed together with their descriptions and assignments. The IR spectrum of 3-methyl-2-phenylpyridine is very similar to that of its complexes in the region 4000–600 cm^{-1} except that the bands due to the aromatic ring vibrations are shifted to higher wavenumbers on formation of the complexes. This suggests that the nitrogen atom of the aromatic ring is coordinated to a metal atom [4]. Further evidence for the proposed tetrahedral and tetragonal environment for the cobalt and copper ions respectively is obtained from the ν(M–Cl) vibrations [1,5]. The ν(Zn–Cl) bands in the zinc complexes occur in the range indicative of zinc complexes having a tetrahedral structure [5].

The fact that the compounds were isolated from solution as powders and not as single crystals meant that no complete structure determination could be made. However, spectroscopic and magnetic data enable us to postulate structures. As previously concluded, the metal ion in the cobalt and zinc complexes is in a tetrahedral environment. Two chloride ions and two 3-methyl-2-phenylpyridine molecules make up the tetrahedral environment around these metal ions. The copper complexes have pseudo-planar structures with long bonds from each copper atom to the halides of other groups as in the structure of bispyridinecopper(II) chloride [6].

The thermal decomposition data are given in Table 4 and Figs. 1–6. The chloro compounds of cobalt and zinc decompose via intermediate compounds to give the metal oxide. The decomposition scheme is:

$$Co(C_{12}H_{10}N)_2Cl_2 \xrightarrow{endo} Co_3(C_{12}H_{10}N)_4Cl_6 \xrightarrow{endo/exo} Co_3O_4$$

$$Zn(C_{12}H_{10}N)_2Cl_2 \xrightarrow{endo} Zn(C_{12}H_{10}N)Cl_2 \xrightarrow{endo/exo} ZnO$$

TABLE 4

Thermal decomposition products

Starting material	Decomposition temperature (°C)	Product	Weight loss (%) [a]	
			Calculated	Found
$Co(C_{11}H_{10}N)_2Cl_2$	158(endo)	$Co_3(C_{12}H_{10}N)_4Cl_6$	24.08	24.05
	242(endo/exo)	Co_3O_4	84.00	83.12
$Co(C_{12}H_{10}N)_2Br_2$	178(endo/exo)	Co_3O_4	86.58	85.13
$Cu(C_{12}H_{10}N)_2Cl_2$	156(endo/exo)	CuO	83.18	83.10
$Cu(C_{12}H_{10}N)_2Br_2$	160(endo/exo)	CuO	88.72	87.27
$Zn(C_{12}H_{10}N)_2Cl_2$	147(endo)	$Zn(C_{12}H_{10}N)Cl_2$	31.70	31.68
	251(endo/exo)	ZnO	82.86	82.50
$Zn(C_{12}H_{10}N)_2Br_2$	168(endo/exo)	ZnO	85.56	85.47

[a] The weight loss in each process is expressed as a percentage of the weight of the initial compound.
endo, endothermic; exo, exothermic.

The other compounds decompose with loss of organic ligand and the halogen to give the metal oxide.

The observed electrical properties of the complexes are summarised in Table 5. The room temperature electrical conductivities for the two copper

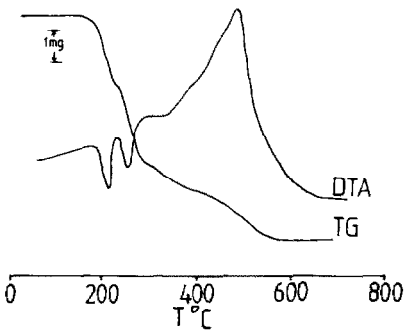

Fig. 1. TG and DTA curves for $Co(C_{12}H_{10}N)_2Cl_2$. Sample weight = 9.48 mg.

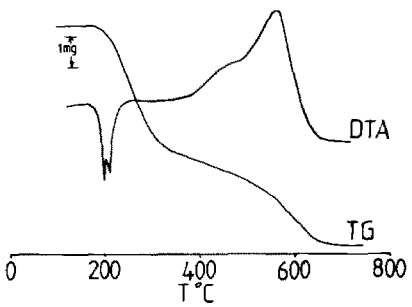

Fig. 2. TG and DTA curves for $Co(C_{12}H_{10}N)_2Br_2$. Sample weight = 9.08 mg.

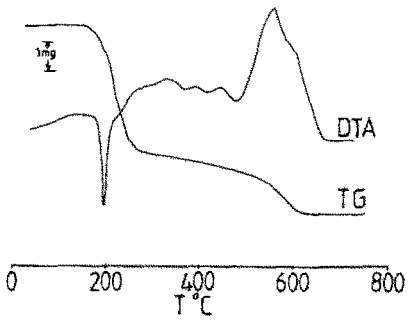

Fig. 3. TG and DTA curves for $Cu(C_{12}H_{10}N)_2Cl_2$. Sample weight = 11.02 mg.

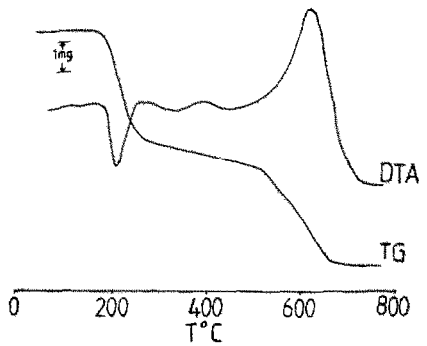

Fig. 4. TG and DTA curves for $Cu(C_{12}H_{10}N)_2Br_2$. Sample weight = 9.43 mg.

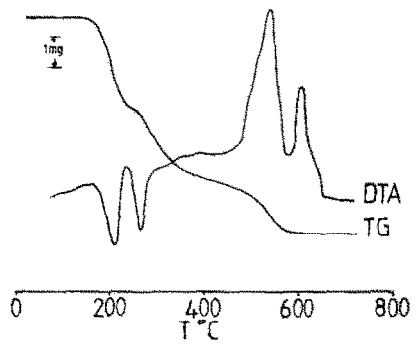

Fig. 5. TG and DTA curves for $Zn(C_{12}H_{10}N)_2Cl_2$. Sample weight = 16.40 mg.

complexes and for $Co(C_{12}H_{10}N)_2Br_2$ are all $2 \times 10^{-13}\ \Omega^{-1}\ m^{-1}$ or less. This is approximately the limit of detection for the apparatus used. The two zinc complexes are much more conducting at room temperature than the other complexes studied, although the reason for this is not apparent. Figure 7 shows that $Zn(C_{12}H_{10}N)_2Cl_2$ is ohmic over the range of applied voltages. For $Zn(C_{12}H_{10}N)_2Br_2$ the I–V characteristic is more complicated (see Fig

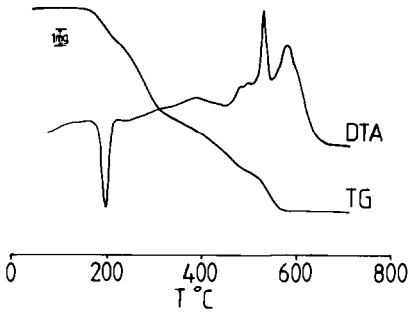

Fig. 6. TG and DTA curves for $Zn(C_{12}H_{10}N)_2Br_2$. Sample weight = 12.87 mg.

TABLE 5

Electrical properties

Compound	σ [a] (Ω^{-1} m^{-1})	m [b]	ΔE [c] (eV)
$Co(C_{12}H_{10}N)_2Cl_2$	1.9×10^{-11}	1.13 ± 0.04	1.90 ± 0.03
$Co(C_{12}H_{10}N)_2Br_2$	2×10^{-13}		
$Cu(C_{12}H_{10}N)_2Cl_2$	2×10^{-13}		
$Cu(C_{12}H_{10}N)_2Br_2$	1×10^{-13}		
$Zn(C_{12}H_{10}N)_2Cl_2$	1.05×10^{-8}	1.00 ± 0.01	1.29 ± 0.04
$Zn(C_{12}H_{10}N)_2Br_2$	1.98×10^{-8}	1.30 ± 0.02	1.54 ± 0.06

[a] Conductivity (σ) at a temperature of 290 K. For $Co(C_{12}H_{10}N)_2Cl_2$ and $Zn(C_{12}H_{10}N)_2Br_2$, where significant departure from ohmic behaviour is involved, the conductivity corresponds to a field of 1×10^4 V m^{-1}.

[b] m is the exponent in the expression $I \propto V^m$ for room temperature current (I) versus voltage (V) characteristics. The value of m is obtained from the gradient of the least-squares-fitted line to a plot of ln I versus ln V.

[c] ΔE is the energy in the equation $\sigma = \sigma_0 \exp(-\Delta E/2kT)$. It is found from the gradient of the least-squares-fitted line to a plot of ln σ versus T^{-1} for heating.

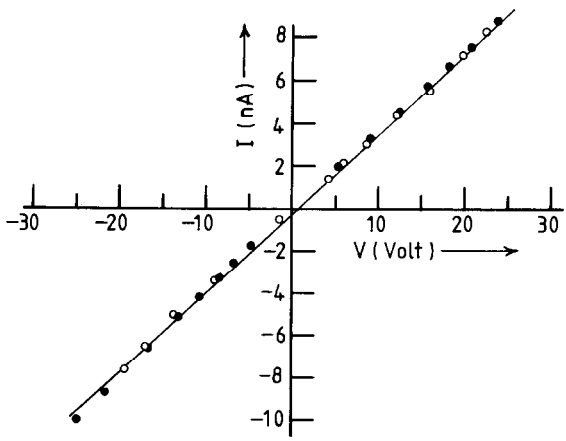

Fig. 7. Current (I) versus voltage (V) for a disc of $Zn(C_{12}H_{10}N)_2Cl_2$ at room temperature. ●, $|V|$ increasing; ○, $|V|$ decreasing.

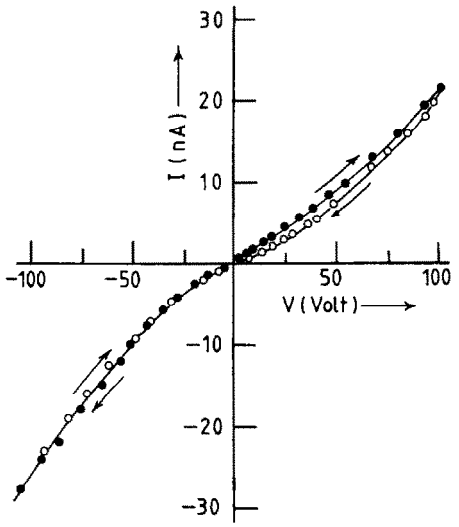

Fig. 8. Current (I) versus voltage (V) for a disc of $Zn(C_{12}H_{10}N)_2Br_2$ at room temperature. ●, $|V|$ increasing; ○, $|V|$ decreasing. Note the hysteresis in the first quadrant.

8); it exhibits hysteresis in the initial polarity (first quadrant) but not under reversed polarity (third quadrant) although curvature of the characteristic remains.

This behaviour has been previously reported [7–9] for other complexes and attributed to a possible distortion of the molecules in an applied electric field with the distortion becoming locked on subsequent removal of the field. For $Co(C_{12}H_{10}N)_2Cl_2$, the I–V characteristics at room temperature, which are not shown, are of the same shape as for $Zn(C_{12}H_{10}N)_2Br_2$. The third column of Table 5 gives values of the exponent m in the expression $|I| \propto |V|^m$, based on data in the third quadrant of the corresponding I–V plot and determined by least-squares fitting of a line to a plot of ln $|I|$ against ln $|V|$. As may be seen from the table, $Zn(C_{12}H_{10}N)_2Br_2$ and to a lesser extent $Co(C_{12}H_{10}N)_2Cl_2$ exhibit values of m exceeding the Ohm's law value of unity and this is due to partial space charge limitation of current.

Figures 9 and 10 respectively show Arrhenius plots, in the form of ln σ versus $10^3/T$, for $Zn(C_{12}H_{10}N)_2Br_2$ and $Co(C_{12}H_{10}N)_2Cl_2$. A similar plot, which is not shown, was obtained for $Zn(C_{12}H_{10}N)_2Cl_2$. For the two zinc complexes the Arrhenius plots are linear over the investigated temperature range and the gradients of the corresponding least-squares-fitted lines give the activation energies ΔE which are listed in Table 5. Assuming that the band model is appropriate, the simplest interpretation of ΔE is that it is the energy gap between valence and conduction bands [10]. For $Co(C_{12}H_{10}N)_2Cl_2$, the Arrhenius plot (see Fig. 10) shows nearly constant conductivity at the lower end of the temperature range and then becomes linear at higher temperatures.

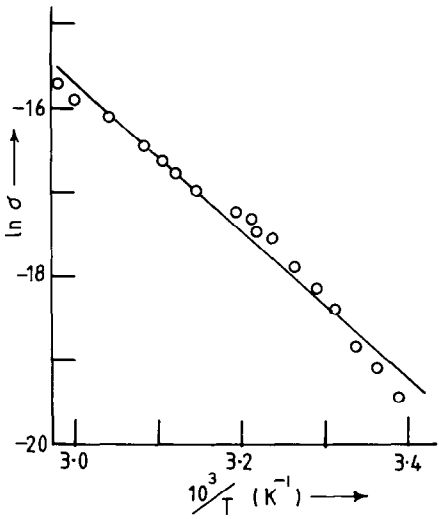

Fig. 9. $\ln \sigma$ versus $10^3/T$ (where σ is the conductivity in units of Ω^{-1} m^{-1} and T is the absolute temperature) for a disc of $Zn(C_{12}H_{10}N)_2Br_2$ during heating. The line is fitted by least squares.

It is suggested that the room temperature conductivity in this complex is governed by donor or acceptor impurity centres that are accidentally present and fully ionised, leading to a range of temperature independence of σ before the temperature is high enough to excite electrons from the valence to

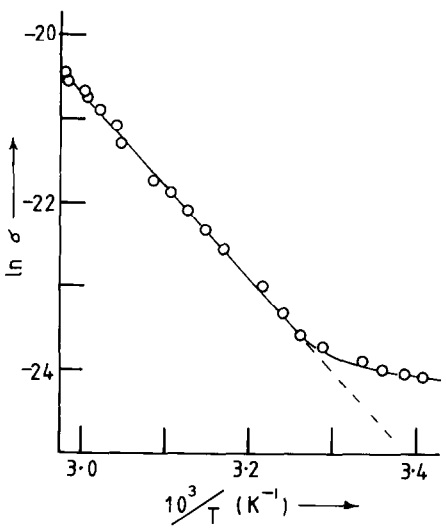

Fig. 10. $\ln \sigma$ versus $10^3/T$ (where σ is the conductivity in units of Ω^{-1} m^{-1} and T is the absolute temperature) for a disc of $Co(C_{12}H_{10}N)_2Cl_2$ during heating. The line for the linear region of the plot is fitted by least squares.

conduction bands. This would explain the shape of the plot in Fig. 10 and would also mean that the measured room temperature conductivity of $Co(C_{12}H_{10}N)_2Cl_2$ is a large overestimate of its room temperature intrinsic conductivity which, by extrapolation of the line, is about 2×10^{-12} Ω^{-1} m^{-1}. Thus, with this correction for suspected impurity in $Co(C_{12}H_{10}N)_2Cl_2$, all of the cobalt and copper complexes have room temperature electrical conductivities some four or more orders of magnitude less than for the zinc complexes.

For those complexes in which the temperature dependence of conductivity was obtained, i.e. $Co(C_{12}H_{10}N)_2Cl_2$ and the two zinc complexes, poor reproducibility of the heating data was obtained during subsequent cooling. The conductivity after returning to room temperature was in all cases less than the initial value. We find this surprising in view of the fact that the maximum temperature reached during the conductivity measurements was far below that corresponding to the onset of thermal decomposition as found from TG/DTA measurements.

REFERENCES

1 J.R. Allan and G.M. Baillie, J. Thermal Anal., 14 (1978) 291.
2 A.B.P. Lever, Inorganic Electronic Spectroscopy, Elsevier, Oxford, 2nd edn., 1984, p. 560.
3 A. Kleinstein and G.A. Webb, J. Inorg. Nucl. Chem., 33 (1971) 405.
4 J.R. Allan, N.D. Baird and A.L. Kassyk, J. Thermal Anal., 16 (1979) 79.
5 J.R. Allan, D.H. Brown, R.H. Nuttall and D.W.A. Sharp, J. Chem. Soc., (1966) 1031.
6 J.A. Dunitz, Acta Crystallogr., 10 (1957) 307.
7 J.R. Allan, A.D. Paton, K. Turvey, H.J. Bowley and D.L. Gerrard, Inorg. Chim. Acta, 149 (1988) 289.
8 J.R. Allan, A.D. Paton, K. Turvey, D.L. Gerrard and S. Hoey, Thermochim. Acta, 146 (1989) 317.
9 J.R. Allan, A.D. Paton and K. Turvey, Thermochim. Acta, 164 (1990) 177.
10 K. Seeger, Semiconductor Physics, Springer, Berlin, 1982, p. 42.